ELSEVIER

Journal of Chromatography A, 724 (1996) 235–250

JOURNAL OF CHROMATOGRAPHY A

Windowless pulsed-discharge photoionization detector Application to qualitative analysis of volatile organic compounds

Gerard Gremaud[a], W.E. Wentworth[a,*], A. Zlatkis[a], Robert Swatloski[b], E.C.M. Chen[b], Stanley D. Stearns[c]

[a]*University of Houston, Department of Chemistry, Houston, TX 77204-5641, USA*
[b]*University of Houston Clear Lake, Houston, TX 77058, USA*
[c]*Valco Instruments Co, P.O. Box 55603, Houston, TX 77255, USA*

Received 14 June 1995; accepted 18 August 1995

Abstract

The effluent from a gas chromatograph was split and directed to four identical windowless photoionization detectors. These detectors use pure helium, helium with Ar (0.64%), Ar (4.15%) and Kr (0.58%) as the discharge gas. The relative ionization cross-sections can be obtained from the ratio of the normalized response using an internal standard. This value is characteristic of the compound and could be used for qualitative analysis. These ratios for 47 compounds encompassing 13 functional groups have been determined and are reported. The values have an average relative standard deviation of 2% for the majority of the compounds. The long-term reproducibility of a smaller set of compounds has been determined and was 0.78–2% relative standard deviation for the Ar detector and 5.6–11.3% (worse cases) where the response of the krypton detector is low.

Keywords: Detectors, GC; Windowless photoionization detector; Photoionization detector; Volatile organic compounds

1. Introduction

The development of sensitive and selective detectors has played a major role in the establishment of chromatography as an unrivaled analytical tool. Chief among the detectors for gas chromatography are the ionization detectors. Recently a pulsed discharge has been used in a helium ionization detector (PDHID) and an electron-capture detector (PDECD). This is accomplished with the same basic hardware by simply changing the potentials and the detector scavenging gas [1,2]. The PDHID was originally designed for the analysis of permanent gases. In this case the column effluent was passed directly through the discharge. Ionization occurs even for Ne which has a higher ionization potential than the major radiation from the He discharge, the so-called Hopfield emission at (13.5–17.7 eV). This indicates that the He metastables played a role in ionization. In order to analyze organic compounds, the effluent was brought in downstream of the discharge region and no response was obtained for Ne. This led to the conclusion that the detector in this configuration was acting as a windowless photoionization detector (PDPID) which was virtually universal [3]. This soon led to the idea of doping the discharge with

*Corresponding author.

0021-9673/96/$15.00
SSDI 0021-9673(95)00921-3

various permanent gases to modify the selectivity of the detector. In a companion paper [4], the use of argon and krypton to provide selectivity is introduced and the concept of using different ionization sources to selectively identify chloroalkenes and chloroalkanes is demonstrated.

The first part of this paper will review briefly the background of photoionization detectors and compare the current detector with the commercially available detectors. Next, the dependence of the emission spectra of the lamps on the concentration of the dopant will be presented. The data will be interpreted in terms of the processes for excitation in the various lamps. Then the effect of the ionization potential of the analytes will be considered as a means of predicting the response of the detectors. The results of the determinations will then be presented and a general procedure for using these results for qualitative identification will be proposed.

The photoionization detector was first described in the early 1960's and subsequently characterized in the following decade [5–7]. In 1971, a windowless PID using microwave excitation of Ne was described [8]. Since 1976, a number of detectors based upon sealed ionization sources have been described and commercialized. This work has fortunately been reviewed and summarized [9–11] so that only a brief comparison of the properties of the commercial lamps and the current sources will be given in this paper.

The emission from the sources in the commercially available photoionization detectors (PID) differs from the sources in the PDPID in two major respects: the transparency of the window and the pressure of the inert gas. The PID sources are sealed lamps so that the transparency of the window plays a critical role in the ionizing emission. The upper limits for the energy available from the Ar and Kr lamps in the PDPID are comparable to those in the PID sources. There is no PID lamp comparable to the He-PDPID detector.

In the He-PDPID, the emission is so far in the vacuum ultraviolet (70–90 nm) that there are no windows available that are transparent at this wavelength, consequently the detector must be windowless. In the case of argon, the atomic resonance emissions at 104.8 nm (11.8 eV) and 106.8 nm (11.6 eV) are at the cut-off wavelength of a lithium fluoride window so that such a window can be used with some attenuation of the intensity. However, in time, the lithium fluoride windows form colored centers due to exposure to UV radiation [10] These color centers will diminish the intensity of the radiation reaching the ionization region. In addition, operation of LiF at high temperatures will cause the cut-off wavelength to shift to longer wavelengths, again attenuating the argon radiation. Thus the argon PID has limited utility and the lifetime of the lamp is significantly less than the Kr or Xe PID lamps [10]. The Kr and Xe lamps used in the PID have magnesium fluoride windows that have sufficient transmission at the corresponding wavelengths to be effective. Of course, any window can be potentially contaminated by condensed analyte and that must be considered in the construction of a PID.

The pressure in the PID sources is low enough so that mainly atomic emission is observed. There is a low-intensity emission from Ar_2^* at 121.6 nm in the PID lamp [10]. In contrast, the concentration of the dopant gas in the PDPID can be varied so that varying amounts of dimer emission relative to atomic emissions can be obtained. This could be used to alter the selective nature of the lamps. Indeed, one of the most attractive features of the PDPID is the ease of switching from one mode to the other by simply changing the discharge gas. This is comparable to the ability to switch from chemical ionization to electron impact ionization in GC–MS.

The selectivity of the various detectors can be predicted by examining a table of ionization potentials for various classes of molecules as shown in Table 1. The table is arranged in order of decreasing ionization potentials (IP) and the compounds are classified according to their functional groups. When a compound has more than one functional group, the compound is classified on the basis of the group having the greatest effect upon the ionization potential. There are fifteen groups of compounds. Examples from thirteen of those groups have been included in this study. The advantage of listing the ionization potentials by groups is that from the highest ionization potential in that group, the photoionization energy required to detect these compounds is immediately known. For example, for the alkanes, the ionization potential for methane is 12.5 eV and ranges down to about 9.5 eV for the higher molecular

mass compounds. Since the argon-doped PDPID emits at a maximum energy of (11.6–11.8 eV), it will not detect methane and will have a small response to ethane but should respond to the higher molecular mass alkanes. The general trend in all groups is that the ionization potential decreases with increasing molecular mass, apparently due to the delocalization of the electrons. By replacing a hydrogen by a hydroxyl to create the alcohol, the ionization potential of even methanol is only 10.6 eV and the ionization potential decreases as the chain length increases. In this case, the argon-doped PDPID will detect all alcohols but the krypton PDPID will not detect methanol and will probably have a small response to ethanol but should respond to the higher alcohols. The ethers, aldehydes, ketones, acids, esters, and amides all have low enough ionization potentials to be detected with the Kr-doped detector. Sulfur compounds and the amines all have low ionization potentials and should be detected in the Kr-doped detector. The ionization potentials of the aromatic and olefinic compounds are all lower than their saturated analog so they can be detected in the Kr-doped PDPID. For example, the ionization potential of hexane is 10.1 eV, whereas that of 1-hexene is 9.45 eV and that of benzene is 9.2 eV. In contrast, the substitution of fluorine increases the ionization potential while that of chlorine slightly lowers the ionization potential and that of iodine significantly lowers the value. For example the ionization potential of methyl iodide is only 9.5 eV compared to the value for methane, 12.5 eV.

In this study, the effluent from the gas chromatograph has been split to four identical detectors in order to determine the relative ionization cross-sections of the different compounds. One of the detectors uses pure He as discharge gas and is therefore a universal detector which serves to normalize the responses of the other three detectors that contain Ar (0.64%), Ar (4.15%) and Kr (0.58%). The different argon concentrations were used to evaluate the effect of the diatomic argon emission. Ultimately this normalized response could be used to identify certain compounds. In the extreme, one compound would have no response in the detector with the lower-energy photons, while the other would give a response. However, if it is possible to accurately measure the relative cross-sections, the magnitude could be used to identify closely eluting compounds. To accomplish this, the response of 47 compounds containing 13 different functional groups has been measured. The compounds selected had sufficient volatility that a gas sample could be injected into the chromatograph. The relative standard deviations for these compounds are reported and show promise for developing an automated system that can be used for qualitative analysis in conjunction with relative retention times.

2. Experimental

The four detectors used throughout this work (Fig. 1) were designed and built in our laboratories. The detector end sections are constructed of 99.8% alumina that has excellent mechanical properties. The discharge region (1.6 mm I.D.) has a smaller I.D. than the other parts (3 mm I.D.) in order to minimize the back diffusion from the column effluent into the discharge region.

Due to the strong tendency towards adsorption on alumina, which can produce tailing peaks, leucosaphire (3 mm I.D.) was used in the ionization region (middle section). The two end flanges and all electrodes (bias, collector, and discharge) were made of stainless steel. The discharge electrodes were platinum-tipped and cemented into the discharge section. Both flanges had a 1/16-inch (ca. 1.6 mm) stainless-steel tubing soldered to them. The tubing on the discharge side was additionally fitted with the discharge gas mixture supply. The tubing on the other side was open to the atmosphere and served as detector outlet as well as the inlet port from the GC capillary column. The parts were sealed with gold O-rings and cemented with high-temperature epoxy glue (Duralco 4703)

The detectors were housed in cavities of a stainless-steel heating block, which was maintained at 322 K to prevent condensation of the samples. This heating block had drilled-out sections through which Selectro-type connectors were passed to reach the bias and collector electrodes. One of the discharge electrodes was grounded and the other was connected to an ignition coil and its ancillary power supply and pulse generator as shown in Fig. 2. These were developed and assembled by the electronics

Table 1
Ionization potentials classified by functional group

	Inorg	Saturates	Unsaturates	Halogen	Sulfur	Alcohols and ethers	Aldehydes and ketones	Acids and esters	Amines, amides	Nitriles	Nitro
24.6	He										
21.6	Ne										
17.7	He_2^*										
15.8	Ar										
15.6	N_2,										
15.4	H_2										
15.3	SF_6										
14.0	Kr,CO,$SiHF_3$										
13.9				CHF_3						CF_3CN	
13.8	CO_2										
13.6	HCN										
13.5	He_2^*										
13.4	C_2N_2			C_2F_6,C_3F_8							
12.9	N_2O			CH_3CF_3							
12.7	HCl,ClF_3										
12.6	H_2O,NOF,ClF			CF_3CF_2Cl							
12.5	CNCl	CH_4		CH_3F							
12.4	O_3			CF_3Cl							
12.3	SO_2,CNCl,BH_3			CF_2Cl_2							
12.2	SiH_2F_2									CH_3CN	
12.1	Xe,O_2										
12.0	HNO_3,$AlCl_3$,SF_4			$CF_2ClCFCl_2$							
11.9	N_2F_4,$SnCl_4$			CHF_2CH_3							
11.8	Ar* SiCl4,BrF			$CFCl_3$,CF_2ClBr						C_2H_5CN	
11.7	HBr,$SiHCl_3$,SiH_4			CH_2FCl,CF_2Cl_2							

11.6 Ar*	BCl_3			$CHCl_2CHCl_2,C_2H_5F$							
11.5	$Cl_2,GaCl_3,PbF_2$	C_2H_6		$CCl_4,CHFCl_2$							
11.4	$B_2H_6,PF_3,COCl_2$		C_2H_2	$CHCl_3,CF_3Br$							
11.3	HNO_2			CH_2Cl_2				HCOOH			
11.2	COS			$CH_3Cl,CHCF$							
11.1	BH_2F	C_3H_8		C_2Cl_6							
11.0	HClO,BrCl			$C_2H_5Cl,1,2\text{-}C_2H_4Cl_2$							CH_3NO_2
10.9	OCl_2			$CH_2ClCH_2ClCH_3$		CH_2O				CH_2CHCN	$C_2H_5NO_2$
10.8				C_3H_7Cl,CH_2ClBr	CH_3OH			HCOOCH$_3$	C_3H_5CN	$n\text{-}C_3H_7NO_2$	
10.7	Rn,PCl_5			C_4H_9Cl				CH_3COOH			$2\text{-}C_3H_7NO_2$
10.6 Kr*	$SiH_3Br,SnBr_2$	C_4H_{10}	$c\text{-}C_4H_8$	$CHCCl,CCl_3Br$				C_2H_5COOH			
10.5	H_2O_2,Br_2,H_2S		C_2H_4	CH_3Br,CH_2Br_2	C_2H_5OH						
10.4	Hl,ClO_2	C_5H_{12}	$1\text{-}C_3H_4$	C_6F_5Cl				$C_4H_9COOOCH_3$			
10.3 Ar_2^*				C_2H_5Br				$CH_3COOOXCH_3$			
10.2	$NH_3,GeCl_2$	$i\text{-}C_5H_{12}$	$1\text{-}C_4H_6$		$n\text{-}C_3H_7OH$	CH_3CHO		C_3H_7COOH	NH_3		
						CH_2CHCHO		C_5H_9COOH			
10.1 Kr*	CS_2,NCl_3	C_6H_{14}		C_2F_4	CS_2 2-C_3H_7OH	C_2H_5CHO		$CH_3COOC_2H_5$			
10.0	AsH_3		$1\text{-}C_6H_{10}$	CH_2CHCl	CH_3OCH_3						
9.95			$1\text{-}C_8H_{12}$		$n\text{-}C_4H_9OH$						

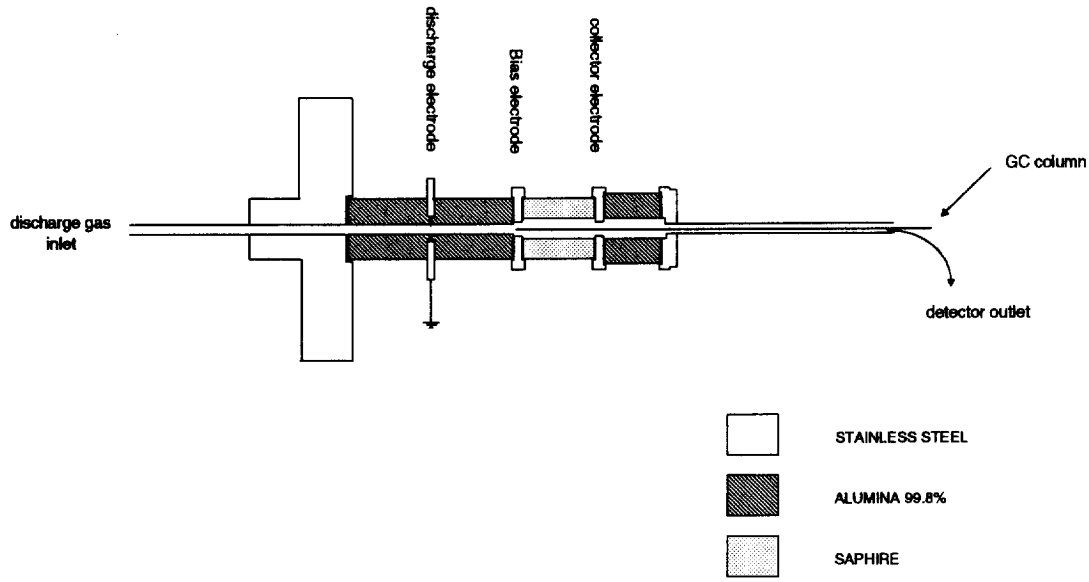

Fig. 1. Schematic diagram of the PDPID.

shop at the University of Houston. In the current experiments, the discharge parameters were chosen as 28-ms pulse width and 220-ms pulse spacing. A d.c. potential of 20 V was supplied to the coil during the 28-ms pulse width. A negative bias potential of 300 V was applied to the cell to direct the photo-induced current towards the collector. The electric current in the cell was measured at the collector electrode with a custom-designed electrometer providing a fixed gain of 10^9. The electrometer collection circuitry consisted of a DT-2770 (Data Translation, Marlboro, MA, USA) interfaced to a DT-2802-4 A/D Intel 486 motherboard. All data were acquired using EZCHROM 5.1 (Scientific Software) chromatographic acquisition software. The A/D board was set to a digital resolution of 19 bits.

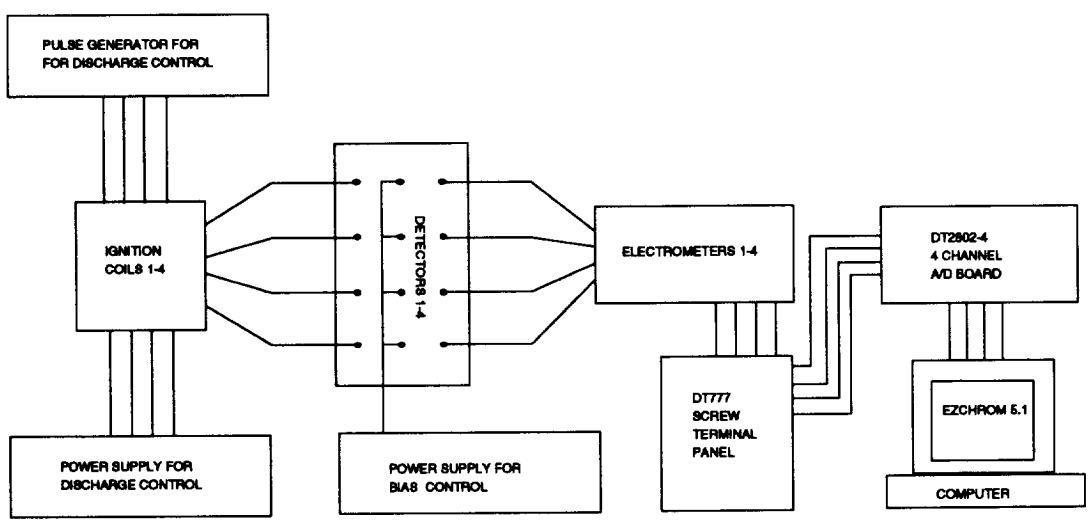

Fig. 2. Schematic of the computer-interfaced GC.

All gases for these experiments were 99.999% purity (five nines) from Trigas (Houston, TX, USA) and were additionally purified by passing them through VICI Helium purifiers (Valco Instruments, Houston, TX, USA) operated on the "bakeout" position (673 K). The pressure-regulated helium flow was split using a VICI four-outlet manifold, and the flow-rates regulated with VICI zero-grease needle valves. Dopant gas (argon or krypton) concentrations were achieved by adding pressure-regulated gases through fixed restrictors prior to a mixing tee downstream of the above described needle valve.

The carrier gas was five-nines helium purified the same way as the discharge gases. The chromatograms were obtained by using a 30 m×0.25 mm I.D., 0.25 μm Rtx-5 column from Restek (Bellefonte, PA, USA). The column effluent was split using a four-way VICI manifold. The transfer lines from this manifold to the individual detectors was made from 0.27 m×0.05 mm×0.05 μm DB-1701 (J&W Scientific, Folsom, CA, USA). These lines have to be precisely the same length to provide equal flow distributions and retention times for all detectors. The carrier gas flow was 3.9 ml/min. All gases were passed through the entire set-up using 1/16-inch stainless-steel tubing (0.03 mm I.D.). The oven of an HP 5880 gas chromatograph was used for these experiments. A schematic diagram of the entire set-up is shown in Fig. 3.

The chemicals were purchased in 99% purity and used as received. The samples were prepared by using a microliter syringe to inject 1–10 compounds and an internal standard into a 100-ml gas-tight syringe (SGE, Austin, TX, USA) filled with either air or helium. The samples were allowed to evaporate completely. Helium was used instead of air when an early eluting solute was difficult to separate from the components of air. The loaded syringe was then fitted to a Valco 6-port valve fitted with a 5-μl loop (Fig. 3). Sample injections were performed in the stream of carrier gas before a GC column. Multiple injections of the same sample were always performed in order to produce statistical data.

The purity of the samples and the actual concentrations in the samples are not critical. In addition, the actual chromatographic ratios (CR) to the various detectors can be removed from the determination by using an internal standard. Thus the only assumption made in determining the relative cross-sections is that the response of the detectors is in the linear region and that the split is not selective so that the amount of the analyte and the amount of the internal standard represent the overall sample eluting from the column and the same split ratio. The use of

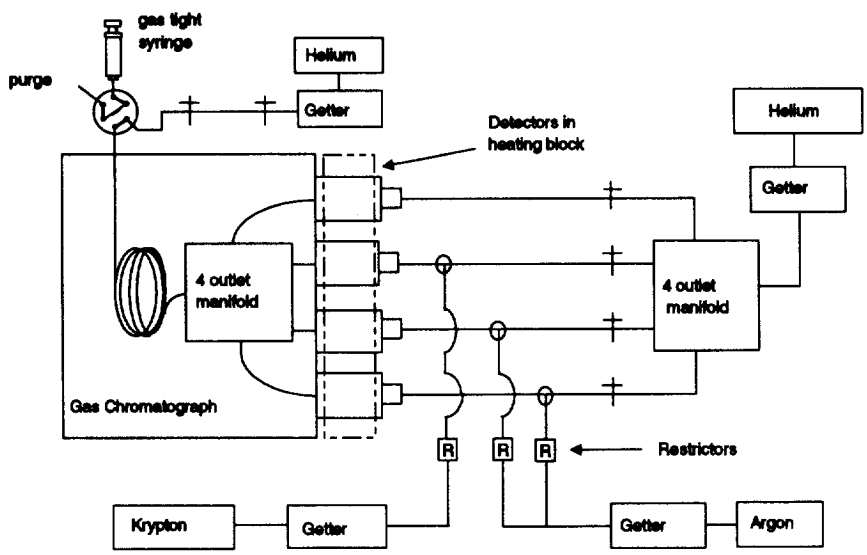

Fig. 3. Schematic diagram of the chromatographic system.

an internal standard will also eliminate variations in peak width so that peak heights could be used for the responses. This can be shown from the following equations.

$$R_{He,X} = k_{He,X} C_X \; R_{He,std} = k_{He,std} C_{std}$$

$$R_{Kr,X} = k_{Kr,X}[CR] C_X \; R_{Kr,std} = k_{Kr,std}[CR] C_{std}$$

where the R values are the responses (areas or heights), C_X is the concentration of the analyte while C_{std} is the concentration of the internal standard and k's are the linear chromatographic factors and are equated to the photoionization cross-sections. By taking the ratio of the absolute responses, the concentration terms cancel and by taking the responses relative to the standard, the response factors are eliminated. If heights are used, then the changes in the widths would be reflected in both the widths of the standard and the analyte so that the experimental quantity of interest is the relative photoionization cross-section (RePIX). The same relationship is applicable to any dopant gas.

$$\text{RePIX} = \frac{(k_X/k_{std})_{Kr}}{(k_X/k_{std})_{He}} = \frac{R_{Kr,X}/R_{Kr,std}}{R_{He,X}/R_{He,std}}$$

This quantity, RePIX, accounts for the concentration dependence and variation in chromatographic properties such as the split ratio and the instrumental properties such as change in the sensitivity in the detectors due to variation in the applied power to the discharge. Certainly over long periods of time, say months, there would be changes in absolute detector sensitivity. Thus we reference the relative responses to benzene, which is assigned a value of 1.0000. Benzene acts as an internal standard. Benzene is used because it has a low ionization potential and is easily detected by all detectors. Other internal standards could be used for this scale provided the relative value to the other standard were known accurately relative to benzene. These values of RePIX should be quite accurate and reasonably reproducible over long periods of time. Since the effluent from the column is split and analyzed by the PDPID, this value should be independent of the usual chromatographic variations such as sample decomposition, leaks and poor chromatographic conditions. The most susceptible component for variation is the composition of the discharge gas and its subsequent emission spectra. A change in gas composition of the doped gases or the purity of the helium could affect the emission spectra and thus even the relative responses.

The emission spectra produced in the discharge was recorded using an Acton 402 monochromator. Normally this is a vacuum monochromator capable of measuring wavelengths as low as 50 nm. A holographic grating allows the measurement of up to 550 nm. Since air absorbs below 190 nm, the monochromator must be evacuated in order to make measurements from 50 to 190 nm. Alternatively, we have purged the monochromator with helium of sufficient purity to allow spectra to be recorded down to 60 nm. Below 60 nm, the helium begins to absorb, primarily through the resonance line at 58.44 nm. Since the PDPID spectrum is of high energy, it is necessary to measure spectra as low as 60 nm. With a vacuum system, a window must be used which limits the spectral region by the transparency of the windows. Lithium fluoride has the greatest transparency at short wavelengths with a cut-off at about 100 nm. As will be seen shortly, the emission spectrum from helium falls completely below the 100 nm cut-off and the atomic emission in the Ar-doped helium occurs at about this cut-off.

Since windows cannot be tolerated in order to record the spectra below 100 nm, the pulsed discharge must be coupled directly to the helium-purged monochromator. This would require purging the slits in the normal operation. However, since the discharge consists of such a very narrow line, we use the discharge as the optical image and eliminate the entrance slit. The discharge is located at the position normally occupied by the entrance slit so that the image is in focus. The Acton 402 monochromator has a 0.2-m optical path with a dispersion of 4.0 nm/mm. The line-like discharge must have a width of about 0.15 to 0.20 mm in order to give a band pass of 0.6–0.8 nm. This resolution is sufficient for recording the emission spectra from the PDPID.

3. Results and discussion

3.1. Spectra

The emission spectra from the pulsed-discharge sources using pure helium and Ar- or Kr-doped helium in the range 60–180 nm are shown in Fig. 4. The helium emission consists only of the broad He_2^* ($A^1\Sigma_u^+$) emission (60–100 nm, 13.5–17.7 eV). The resonance radiation at 21.2 eV (58.44 nm) from the atomic transition ($2^1P \rightarrow 1^1S$) is self absorbed since the helium is at 1 atm pressure (101.325 MPa). Argon- and krypton-doped helium give both the atomic resonance radiation and the dimer continuum emission. The atomic resonance radiation actually consists of two lines. In the case of argon, these lines are closely spaced, 104.8 and 106.6 nm, and are not completely resolved with the Acton monochromator. The resonance lines are broadened which could be due to the high pressure and/or the mode of excitation.

In another study, we determined the emission intensity–time profile arising from various excited species [12]. Both the argon and krypton emissions occur later than the He_2^* triplet emission. Thus, we think that the excitation of the Ar and Kr atomic resonance emissions arise from:

$$Ar + He_2^*(a^3\Sigma_u^+) \rightarrow Ar^*(4^3P) + 2He(1^1S)$$

$$Kr + He_2^*(a^3\Sigma_u^+) \rightarrow Kr^*(5^3P) + 2He(1^1S)$$

The time delay could allow the excited species to diffuse out of the discharge region that would also broaden the spectral image. In general, the atomic emissions from N/N_2 or H/H_2O are more narrow than the Ar and Kr atomic lines. The diatomic continuum emissions arise from the subsequent reactions:

$$Ar + Ar^*(4^3P) \rightarrow + Ar_2^*(a^3\Sigma_u^+)$$

$$Kr + Kr^*(5^3P) \rightarrow + Kr_2^*(a^3\Sigma_u^+)$$

The resulting broad band emission from the excited diatomic species arises from:

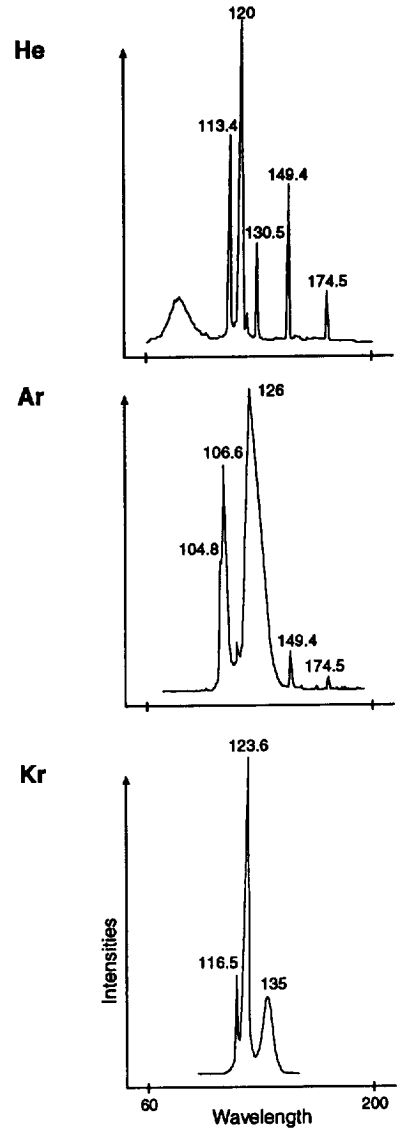

Fig. 4. Spectra of pure helium, argon-doped helium and krypton-doped helium.

$$Ar_2^*(a^3\Sigma_u^+) \rightarrow 2Ar + h\nu(9.28 - 10.24\ eV)$$

$$Kr_2^*(a^3\Sigma_u^+) \rightarrow 2Kr + h\nu(8.11 - 8.87\ eV)$$

similar to the Hopfield emission from He_2^* ($A^1\Sigma_u^+$) [13]. Since the Ar_2^* and Kr_2^* are formed from a

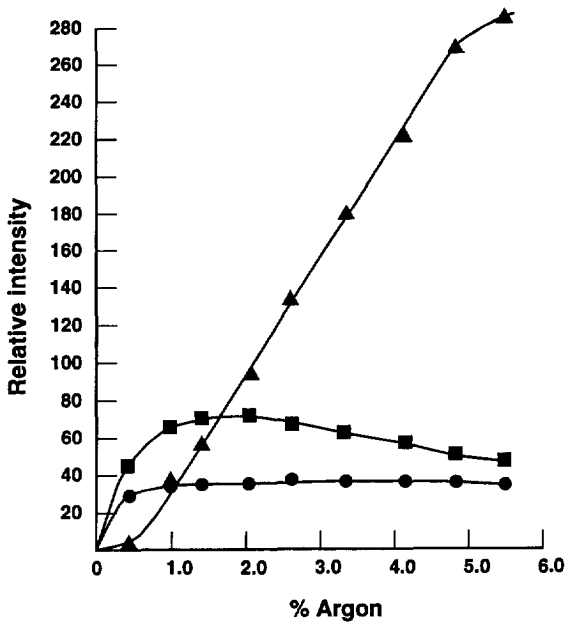

Fig. 5. Relative intensities of mono and diatomic emission as a function of % argon: (●) 104.8 nm, (■) 106.6 nm, (▲) 121–133.6 nm.

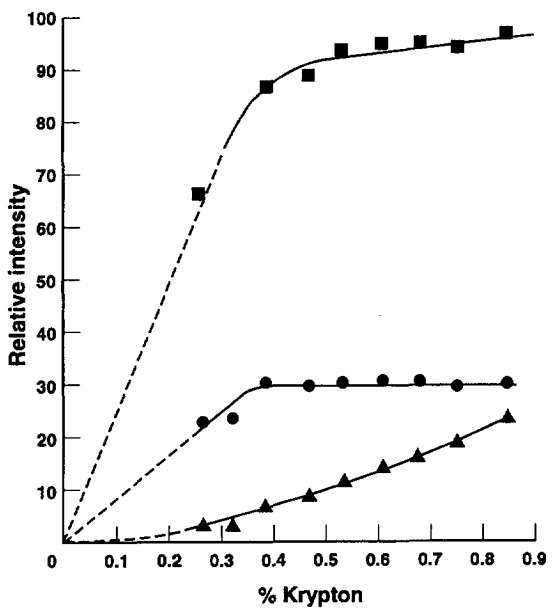

Fig. 6. Relative intensities of mono and diatomic emission as a function of % krypton: (●) 116.5 nm, (■) 123.6 nm, (▲) 135 nm.

second-order reaction, the emission intensity of the dimeric excimer increases with the concentration of Ar and Kr. The intensity of the atomic emission also increases at low concentrations of Ar and Kr but then becomes relatively constant. This is expected since the excited atomic species are depleted in the reaction to produce the dimers. By varying the concentration of the dopant, the atomic and diatomic emissions can be varied and could be used in selective ionization.

The emission spectra from the Ar- and Kr-doped He have been recorded as a function of dopant concentration. The intensities of the atomic and diatomic emission as a function of percentage dopant are shown in Fig. 5 and Fig. 6. The atomic emissions from argon at 104.8 and 106.6 nm reach a maximum intensity at about 1% and then remain approximately constant. The 106.6-nm line decreases slightly when the concentration of the argon is above 2%. On the other hand, the diatomic emission in the range 121–138 nm increases almost linearly with concentration from 1 to 6% argon. Both the increases in the dimer emission and the leveling of the atomic emissions are as expected since the dimer is formed from the monomer in a second-order process. A similar situation occurs for the krypton emission except that the intensity of the atomic emission begins to level off at about 0.4–0.5%. Because of the cost of krypton and because our source of krypton was a mixture of Kr in He, we have not investigated the emission of Kr above 0.9% Kr. However, in Fig. 6, the dimer emission at 135 nm increases in intensity as the krypton concentration is increased.

3.2. Relative photoionization cross-sections (RePIX)

The relative values of the responses (RePIX, Bz) (see Section 2 for the details of the calculation) are given in Tables 2 and 3. In Table 2, the values are given in the order of the RePIX (4.15% Ar) values. At least five chromatograms were run for each compound so that the reported values are the average of these runs. The standard deviation and relative standard deviations are given in Table 2. In the cases where no values are given, the response was too small to be quantitated but five attempts were made.

Table 2
Relative photoionization cross-sections (RePIX) sorted by RePIX(4.15% Ar)

Compound	I.P. (eV)	RePIX (4.15% Ar)	R.S.D. (%)	RePIX (0.64% Ar)	R.S.D. (%)	RePIX (0.58% Kr)	R.S.D. (%)
CH_3CN	12.19±0.005	0.006±0.0005	6.30	0.019±0.001	3.76	0.011±0.0005	4.25
CCl_2FCF_2Cl	11.99±0.02	0.019±0.001	5.54	0.026±0.002	7.26	0.019±0.001	5.15
CCl_4	11.47±0.01	0.306±0.001	0.22	0.327±0.001	0.22	0.029±0.003	11.51
3-Pentanone	9.31±0.01	0.355±0.003	0.78	0.316±0.006	1.83	0.406±0.016	3.94
$CHCl_3$	11.37±0.02	0.401±0.001	0.36	0.433±0.002	0.47	0.028±0.003	11.97
Acetone	9.71	0.403±0.007	1.80	0.393±0.013	3.32	0.571±0.009	1.56
2-Propanol	10.12±0.08	0.441±0.002	0.45	0.458±0.005	1.15	0.092±0.008	8.14
Butyraldehyde	9.84±0.02	0.476±0.008	1.70	0.500±0.009	1.88	0.205±0.023	11.15
Ethyl ether	9.51±0.03	0.480±0.006	1.21	0.535±0.003	0.50	0.309±0.009	2.78
Tetrahydrofuran	9.41±0.02	0.528±0.061	11.58	0.612±0.017	2.84	–	
Methyl-*tert.*-butyl ether	9.24	0.533±0.003	0.53	0.562±0.004	0.75	0.327±0.003	0.84
Triethylamine	7.50	0.539±0.024	4.52	0.307±0.018	5.84	0.432	–
2-Chloropropane	10.78±0.02	0.543±0.008	1.45	0.620±0.011	1.83	–	–
$CF_3C_6H_5$	9.68±0.004	0.566±0.001	0.18	0.617±0.003	0.51	0.481±0.011	2.24
CH_3CCl_3	11.00	0.601±0.001	0.23	0.679±0.002	0.32	–	–
Propyl ether	9.27±0.05	0.626±0.002	0.32	0.681±0.006	0.84	0.151±0.013	8.76
1-Propanol	10.22±0.03	0.638±0.006	0.88	0.645±0.010	1.53	0.084±0.010	12.34
n-Pentane	10.35±0.01	0.649±0.013	2.01	0.757±0.010	1.31	–	–
Propyl formate	10.52±0.02	0.663±0.003	0.48	0.726±0.008	1.09	–	–
1-Pentanol	10.00±0.03	0.667±0.011	1.72	0.697±0.008	1.20	–	–
n-Heptane	9.92±0.05	0.686±0.006	0.91	0.789±0.002	0.29	–	–
n-Hexane	10.13	0.701±0.006	0.86	0.827±0.001	0.14	0.063±0.005	–
CH_2ClCH_2Cl	11.06	0.725±0.003	0.47	0.833±0.009	1.14	0.030	8.38
CH_2Cl_2	11.32±0.01	0.780±0.003	0.35	0.879±0.001	0.17	0.035±0.005	14.48
2-Nitropropane	10.71±0.05	0.795±0.006	0.77	0.937±0.011	1.15	–	–
1-Hexene	9.44±0.04	0.795±0.004	0.55	0.877±0.001	0.16	0.334±0.007	2.15
Nitromethane	11.02±0.04	0.817±0.009	1.09	0.903±0.024	2.67	0.187±0.018	9.47
Cyclohexane	9.86±0.03	0.840±0.007	0.81	0.979±0.010	1.05	0.178±0.005	2.71
1-Bromobutane	10.13	0.842±0.001	0.17	0.961±0.003	0.31	0.166±0.007	4.33
Ethyl benzene	8.77±0.01	0.905±0.013	1.43	0.943±0.017	1.76	0.533±0.019	3.54
Ethyl sulfide	8.43±0.01	0.907±0.003	0.31	0.957±0.006	0.67	0.557±0.011	1.91
o-Xylene	8.56±0.01	0.961±0.012	1.24	1.023±0.012	1.21	0.607±0.019	3.16
p-Xylene	8.44±0.01	1.021±0.015	1.50	1.083±0.017	1.53	0.690±0.018	2.60
Toluene	8.82±0.01	1.034±0.005	0.50	1.066±0.011	1.02	0.797±0.015	1.82
m-Xylene	8.56±0.01	1.039±0.018	1.70	1.095±0.011	1.02	0.645±0.021	3.27
Propylamine	8.78±0.02	1.046±0.066	6.29	0.843±0.042	4.99	–	–
Cyclohexene	8.94±0.01	1.049±0.007	0.71	1.173±0.009	0.74	0.383±0.009	2.33
$CHClCCl_2$	9.47±0.01	1.103±0.006	0.58	1.162±0.007	0.65	0.685±0.006	0.94
cis-ClCHCHCl	9.66±0.01	1.171±0.009	0.79	1.305±0.010	0.75	0.731±0.021	2.82
Allylsulfide	No V.	1.194±0.004	0.36	1.235±0.025	1.99	0.826±0.063	7.66
ClC_6F_5	9.72±0.02	1.195±0.007	0.56	1.366±0.008	0.58	0.345±0.036	10.49
C_6F_6	9.91	1.209±0.022	1.80	1.282±0.016	1.26	0.229±0.026	11.29
C_2Cl_4	9.32	1.322±0.006	0.42	1.419±0.014	0.96	0.696±0.005	0.79
C_6H_5Cl	9.06±0.02	1.411±0.014	0.96	1.508±0.020	1.32	0.914±0.072	7.91
Ethyl iodide	9.35	1.456±0.007	0.46	1.471±0.007	0.49	1.430±0.017	1.09
CH_2Br_2	10.50±0.02	2.110±0.017	0.78	2.372±0.023	0.96	0.181±0.010	5.62
CS_2	10.07±0.002	2.402±0.016	0.68	2.612±0.004	0.14	0.521±0.005	1.04

In Table 3, the values are given in the order of ionization potentials. The ionization potentials are also given in Table 2 for convenience.

From Table 3, when the ionization potential of the compound is greater than 11.8 eV, the RePIX(Ar) is small or negligible. Starting with CCl_4 with an

Table 3
Relative photoionization cross-sections (RePIX) sorted by ionization potential

Compound	I.P. (eV)	RePIX (4.15% Ar)	RePIX (0.64% Ar)	RePIX (0.58% Kr)
CH_3CN	12.19±0.005	0.006	0.019	0.011
CCl_2FCF_2Cl	11.99±0.02	0.019	0.026	0.019
CCl_4	11.47±0.01	0.306	0.327	0.029
CH_2Cl_3	11.37±0.02	0.401	0.433	0.028
$CHCl_2$	11.32±0.01	0.780	0.879	0.035
CH_2ClCH_2Cl	11.06	0.725	0.833	0.030
Nitromethane	11.02±0.04	0.817	0.903	0.187
CH_3CCl_3	11.00	0.601	0.679	–
2-Chloropropane	10.78±0.02	0.543	0.620	–
2-Nitropropane	10.71±0.05	0.795	0.937	–
Propyl formate	10.52±0.02	0.663	0.726	–
CH_2Br_2	10.50±0.02	2.110	2.372	0.181
n-Pentane	10.35±0.01	0.649	0.757	–
1-Propanol	10.22±0.03	0.638	0.645	0.084
n-Hexane	10.13	0.701	0.827	0.063
1-Bromobutane	10.13	0.842	0.961	0.166
2-Propanol	10.12±0.08	0.441	0.458	0.092
CS_2	10.07±0.002	2.402	2.612	0.521
1-Pentanol	10.00±0.03	0.667	0.697	–
n-Heptane	9.92±0.05	0.686	0.789	–
C_6F_6	9.91	1.209	1.282	0.229
Cyclohexane	9.86±0.03	0.840	0.979	0.178
Butyraldehyde	9.84±0.02	0.476	0.500	0.205
ClC_6F_5	9.72±0.02	1.195	1.366	0.345
Acetone	9.71	0.403	0.393	0.571
$CF_3C_6H_5$	9.68±0.004	0.566	0.617	0.481
cis-ClCHCHCl	9.66±0.02	1.171	1.305	0.731
Ethyl ether	9.51±0.03	0.480	0.535	0.309
$CHClCCl_2$	9.47±0.01	1.103	1.162	0.685
1-Hexene	9.44±0.04	0.795	0.877	0.334
Tetrahydrofuran	9.41±0.02	0.528	0.612	–
Ethyl iodide	9.35	1.456	1.471	1.430
C_2Cl_4	9.32	1.322	1.419	0.696
3-Pentanone	9.31±0.01	0.355	0.316	0.406
Propyl ether	9.27±0.05	0.626	0.681	0.151
Methyl-*tert.*-butyl ether	9.24	0.533	0.562	0.327
C_6H_5Cl	9.06±0.02	1.411	1.508	0.914
Cyclohexene	8.94±0.01	1.049	1.173	0.383
Toluene	8.82±0.02	1.034	1.066	0.797
Propylamine	8.78±0.01	1.046	0.843	–
Ethylbenzene	8.77±0.01	0.905	0.943	0.533
m-Xylene	8.56±0.01	1.039	1.095	0.645
o-Xylene	8.56±0.01	0.961	1.023	0.607
p-Xylene	8.44±0.01	1.021	1.083	0.690
Ethyl sulfide	8.43±0.01	0.907	0.957	0.557
Triethylamine	7.50	0.539	0.307	0.432
Allylsulfide	No V.	1.194	1.235	0.826

ionization potential of 11.47 eV, the RePIX is 0.306 and continues to be high for all compounds with a lower ionization potential. The values range to 2.40 for CS_2.

Similarly for the values of RePIX(Kr), the response is small for compounds with ionization potentials above 10.1 eV and certainly for compounds with ionization potentials above 10.6 eV.

Recall that the atomic emission at 10.1 eV was much more intense than the emission at 10.6 eV. For most of the compounds with ionization potentials less than 10.1, the RePIX is significant, ranging to a high of 1.430 for ethyl iodide. For the compounds with ionization potential above 10.6 eV, there are a few compounds with a small but measurable RePIX. In addition, for some compounds with low ionization potentials, the responses could not be measured. In the case of the molecules with higher ionization potentials, the extra energy could be supplied by reaction of excited species or could be the result of bond formation. The low response for the compounds with low ionization potentials could be due to chromatographic problems. These exceptions are under investigation.

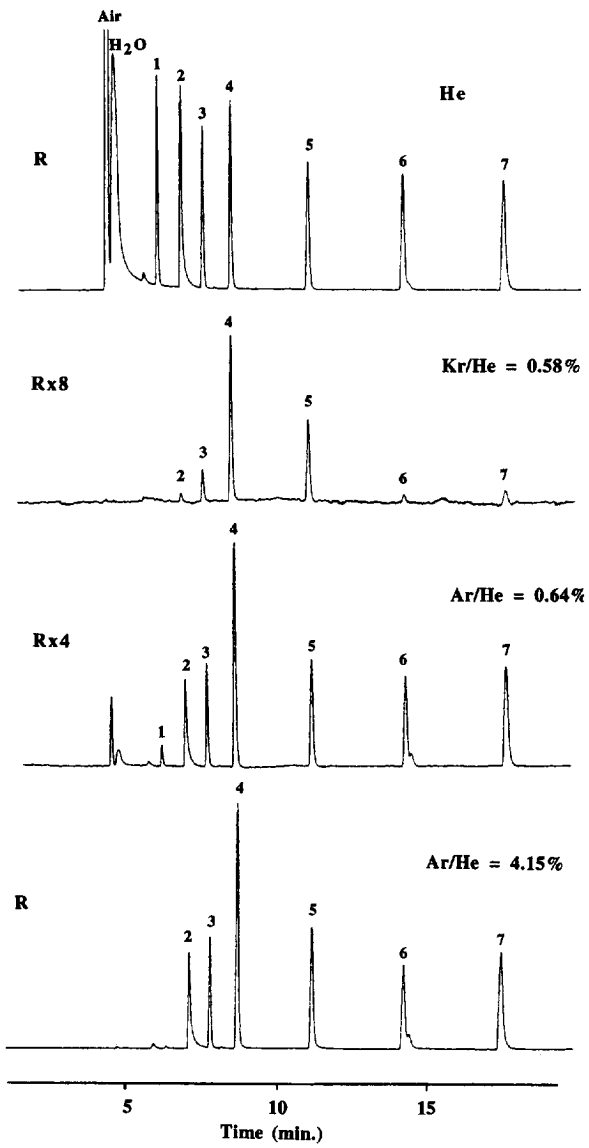

Fig. 7. Comparison of responses in pure helium, helium+0.58% krypton, helium+0.64% argon, helium+4.15% argon. Peaks: 1=freon 113, 2=1-propanol, 3=1-hexene, 4=ethyl iodide, 5=benzene, 6=heptane, 7=1-bromobutane.

Tables 1–3 are useful in predicting the selectivity of the PDPID. One detector will give adequate response for some compounds and at the same time possibly eliminate interference from other compounds in the mixture. Particularly noteworthy is the elimination of a response to water and air by using the 4.15% Ar-doped PDPID. This is specially important for environmental analysis of air and water samples. Also the response of a certain class of compounds can be enhanced and at the same time minimize the response to other classes of compounds. For example, the Kr-doped PDPID can be used to selectively measure aldehydes, ketones, and aromatics in the presence of aliphatic hydrocarbons or fluoro compounds. Table 1 is especially useful for this purpose. This selectivity is illustrated by the chromatograms shown in Fig. 7.

Tables 2 and 3 can be used to investigate the objective of using the RePIX for qualitative analyses. There are three sets of RePIX values for each compound. The question is simply are these unique to a given compound so that it can be identified by this set of numbers within the experimental errors. In order to see if these three values define or distinguish each compound, we can first search through Table 3 to see if the RePIX(Ar 4.15%) values are different enough for each compound. When there is an overlap, we then examine the RePIX(Ar 0.64%) and RePIX(Kr 0.58%) values to see if they are different based upon some statistical evaluation.

An alternative to this search routine is to examine a graph of RePIX(Kr 0.58%) and RePIX(Ar 0.64%) versus RePIX(Ar 4.15%) to see if there is a correlation or non-correlation between the two sets of results. Such graphs are shown in Fig. 8 and Fig. 9 with the respective error bars. From Fig. 8, the RePIX(Ar 0.64%) and RePIX(Ar 4.15%) are highly correlated as indicated by the linear relationship between these values. Thus a single parameter can be used to determine the RePIX(Ar 0.64%) from the measured values of RePIX(Ar 4.15%). In other

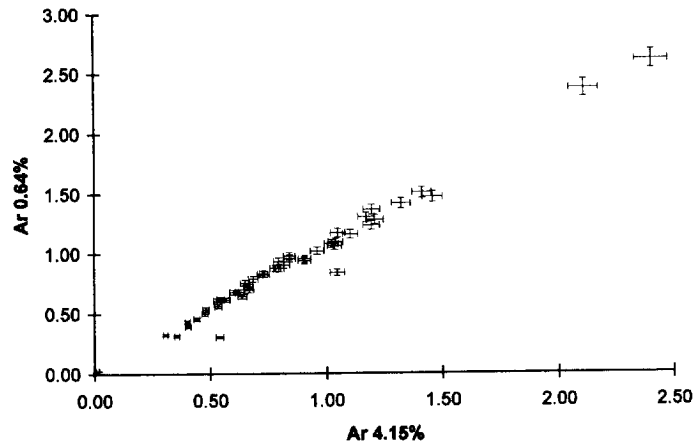

Fig. 8. Relative response for argon (0.64%) versus relative response for argon (4.15%).

words, the two Ar PDPID responses are not independent and only one set of relative responses can be used for qualitative identification of a compound. There are four exceptions where the data points deviate significantly from the straight line. In Fig. 8, the two points falling below the line are propylamine and triethylamine. Since these compounds have exceptionally low ionization potentials, it is not surprising that the response to the Ar(4.15%) PDPID would be greater where a significant portion of the emission is at a low energy (9.2–10.2 eV). Unless other deviations are found, there seems to be little advantage in using two Ar-doped PDPIDs.

In contrast to the correlation found in Fig. 8, there appears to be very little correlation between the RePIX(Kr 0.58%) and the RePIX(Ar 4.15%) values. Thus these data could be used to contribute to the identification of a compound. With only two relative responses available, it would appear that these values should be combined with relative retention times to make this qualitative identification practical. This was not done in this study but will be included in

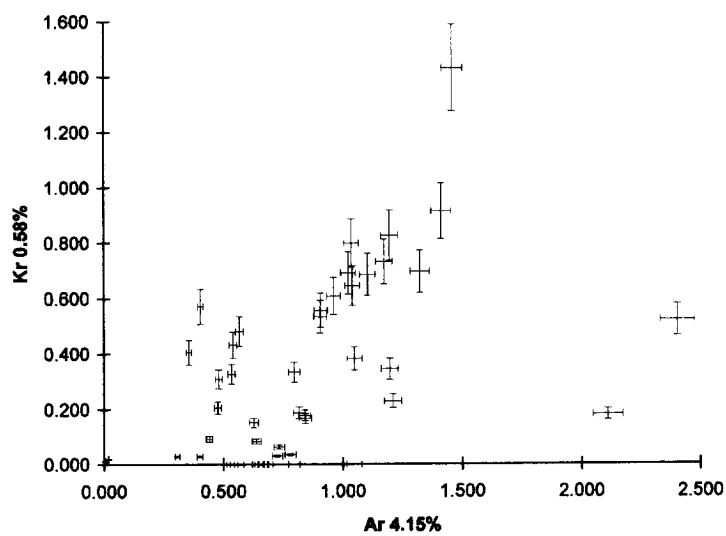

Fig. 9. Relative response for krypton (0.58%) versus relative response for argon (4.15%).

future investigations. This is especially important for those compounds with higher ionization potentials that have a low response to the Kr-doped PDPID. In Fig. 9, there are some data points that are not separated within the error so that relative retention time would be essential.

The purpose of splitting the effluent into the four detectors was to obtain a greater precision in the relative responses from the PDPIDs. From Table 2, the errors in the RePIX(Ar) average less than $0.9 \pm 0.7\%$ The majority of the values are from 0.5 to 2%. There are three outliers (greater than 4% relative standard deviation) with a significant response: tetrahydrofuran, triethylamine, and propylamine. These did not chromatograph well. The relative errors in the Kr-doped PDPID vary with the magnitude of the response. Generally the errors are greater than those for the Ar-doped detector, the average value is in the range of 4%. However, there are some values which are as high as 12%.

The magnitude of the errors in the relative responses is critical in differentiating between two sets of values for qualitative identification of the compounds. In principle, no two compounds would be expected to have precisely the same values of RePIX in the Ar and Kr PDPID. Certainly, the absorption spectra and internal conversion to the photoionized state are different for different compounds, even those of similar structure. However, the relative responses can not be differentiated if the difference between the relative responses is less than the errors associated with them. As we gain experience with these detectors, we expect to obtain more precise relative values.

The errors quoted in Table 2 are those derived from data taken over a somewhat short period of time, within a few hours. These would be appropriate if the detectors were calibrated on a daily basis. To check the stability of these measurements over a longer time period (weeks) we carried out a study using pentane, hexafluorobenzene and dibromomethane, and measured the RePIX values. The relative errors ranged from 0.78% to 2% for the Ar detector and from 5.6 to 11.3% for the Kr-doped detector and these are comparable to the short-term reproducibility.

The use of the RePIX values for qualitative analysis is illustrated in Fig. 10. The compounds are divided into two groups based upon their response in the Kr-doped detector for RePIX(Kr). Values less than 0.2 are placed in one group, containing 25 compounds. The other 22 compounds can be further divided into a group with RePIX(Kr) between 0.2 and 0.45 and a group with a value larger than 0.45. The RePIX(Ar 4.15%) values for these compounds are used as the x-axis. The y-axis is a gaussian with a magnitude of 1 and a width equal to experimental standard deviation. This is analogous to a mass spectrum where all of the potential masses are shown with their respective resolution at equal intensities. The greatest magnitude is 2, indicating one overlap within the error. The large errors for tetrahydrofuran and propyl amine are clearly indicated. An improvement in the precision of these values would help in the identification. In the cases of overlap, the relative retention times would be very useful. Frequently, the RePIX values are similar for a class of compounds, i.e. ketones or alcohols. In these cases, the relative

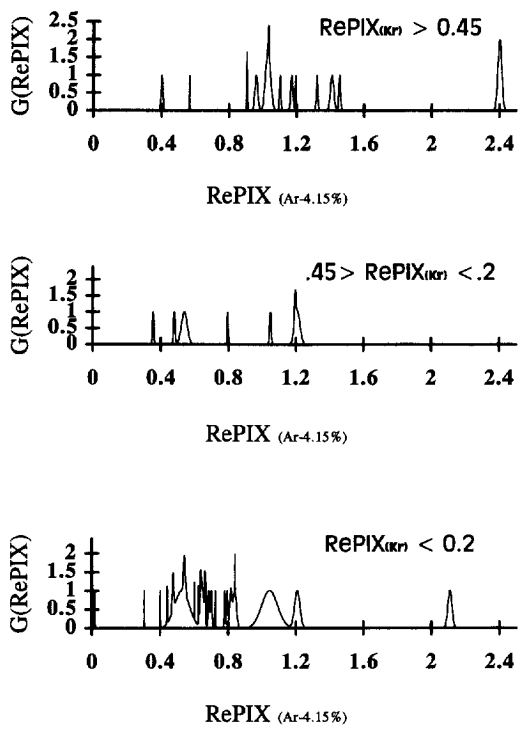

Fig. 10. Gaussian error distribution of individual G(RePIX) versus relative photoionization cross-section [RePIX(Ar 4.15%)] at various RePIX(Kr 0.58%) values.

retention times would be quite different since the compounds would contain a different carbon chain length.

4. Conclusions

The effluent from a gas chromatograph was split and directed to four identical windowless photoionization detectors. These detectors use pure helium, and helium with Ar(0.64%), Ar(4.15%) and Kr(0.58%) as the discharge gas. The relative photoionization cross-sections (RePIX) have been obtained from the ratios of the normalized response of a compound in the Ar or Kr detector, to the normalized response of the same compound in the pure helium detector. This RePIX value is characteristic of the compound and could be used for qualitative analysis. The RePIX values for 47 compounds encompassing 13 functional groups have been determined and are reported. The relative responses using the two different argon concentrations are highly correlated. Consequently, for most compounds, only the relative responses of one of the argon concentrations can be used effectively for qualitative identification. Conversely the relative responses for the krypton-doped and the argon-doped helium detectors are uncorrelated and the two relative values could be used to assist in qualitative identification of an analyte.

The RePIX values have an average relative standard deviation of 2% for the majority of the compounds. The long-term reproducibility of a smaller set of compounds has been determined and was 0.78–2% relative standard deviation for the Ar detector and 5.6–11.3% (worse cases) where the response of the krypton detector is low. This is comparable to the short-term variation. The relative standard deviations show promise for developing an automated system that can be used for qualitative analysis in conjunction with relative retention times.

Acknowledgments

The authors wish to thank Larry Sims from the electronics shop and N. Helias and K. Sun from the University of Houston for their assistance in this study. This research was carried out in collaboration with Valco Instruments (Houston, TX, USA). This research was supported by the Swiss National Science Foundation, Valco Instruments Co., the Robert A. Welch Foundation (Grant E-095 and UHCL Chemistry Departmental Grant), Texas Advanced Technology Development and Transfer Program 1993 (Project Number 00365-076), and NASA-JSC (sponsor ID: NAG 9-742)

References

[1] W.E. Wentworth, S.V. Vasnin, S.D. Stearns and C.J. Meyer, Chromatographia, 34 (1992) 219.
[2] W.E. Wentworth, E.D. D'Sa, H. Cai and S.D. Stearns, J. Chromatogr. Sci., 30 (1992) 478.
[3] W.E. Wentworth, H. Cai and S.D. Stearns, J. Chromatogr. A, 688 (1994) 135.
[4] W.E. Wentworth, Y. Li and S.D. Stearns, J. High Resolut. Chromatogr., in preparation.
[5] D.C. Meloan, Anal. Chem., 37 (1965) 389.
[6] J.G.W. Price, D.C. Fenimore, P.G. Simmonds and A. Zlatkis, Anal. Chem., 40 (1968) 541.
[7] J.N. Driscoll and F.F. Spaziani, Anal. Instrum., 13 (1974) 111.
[8] R.R. Freeman and W.E. Wentworth, Anal. Chem., 43 (1971) 1987.
[9] J.N. Driscoll, CRC Crit. Rev. Anal. Chem., 17 (1986) 193.
[10] J.N. Davenport and E.R. Adlard, J. Chromatogr., 230 (1984) 13.
[11] J.N. Driscoll, in H.H. Hill and D.G. McMinn (Editors), Detectors for Capillary Chromatography, Chemical Analysis Series, Vol. 121, Wiley, New York, 1992, Ch. 4.
[12] W.E. Wentworth, S. Wiedeman, Y. Qin, J. Madabushi and S.D. Stearns, J. Appl. Spectrom., in press.
[13] E. Morikawa, R. Reiniger, P. Gurtler, V. Saile and P. LaPorte, J. Chem. Phys., 91 (1989) 1469.